

Critical statistics in a KAM system

C. E. Creagh, G. Hur and T. S. Monteiro
 Department of Physics and Astronomy, University College London,
 Gower Street, London WC1E 6BT, United Kingdom
 (Dated: May 24, 2019)

We report a theoretical study of a chaotic KAM system, in a regime where the eigenstates have generic localization properties resulting from transport through classical cantori. We find eigenvalue statistics of a form analogous to the critical statistics of a Metal-Insulator Transition in a disordered system: the variances have a linear form $\langle \langle L \rangle \rangle^2 \propto L^{1-D_2}$, where D_2 is a fractal dimension which characterizes the wavefunctions. The nearest-neighbour statistics assume an invariant form which, despite a fully chaotic classical phase-space, is far from GOE.

PACS numbers: 32.80.Pj, 05.45.Mt, 05.60.-k

Random Matrix Theory (RMT) is used to describe the quantum spectral fluctuations of classically chaotic systems as well as disordered metals in the delocalized regime. For the well-studied orthogonal symmetry class, the level spacings distributions are approximated by the well-known GOE (Gaussian Orthogonal Ensemble) form $P(s) \propto \exp(-\frac{1}{4}s^2)$. For integrable systems, as well as disordered conductors after Anderson localization, one finds instead uncorrelated Poisson statistics, with $P(s) \propto \exp(-s)$. But there is much current interest in so-called 'critical' statistics [1, 2], intermediate between those of RMT and the Poisson. These were extensively investigated in relation to the Metal-Insulator Transition (MIT) occurring in 3-dimensional metals. A new universal distribution termed 'semi-Poisson', $P(s) \propto \exp(-2s)$ with a long-range Poisson tail but the short range repulsion of the RMT form [3] has been associated with the MIT [4]. For critical statistics a very interesting connection has been established between the multifractal characteristics of the wavefunctions and those of the spectral fluctuations [4, 5]: the number variances of the spectra are linear $\langle \langle L \rangle \rangle^2 \propto L$ for $L \gg 1$. The slope, $\gamma = 2(1 - D_2)$, was shown to be related to a fractal dimension D_2 obtained from the second moment of the wavefunction and to d , the spatial dimension of the system. For integrable dynamics, in contrast, $\langle \langle L \rangle \rangle^2 \propto L$ while for a GOE, $\langle \langle L \rangle \rangle^2 \propto \ln(L)$.

There are systems without disorder such as the Coulomb billiard [3] where the dynamics would be integrable were it not for a discontinuity or small scattering centre which instantly breaks all classical phase-space barriers. Such pseudo-integrable systems have also been found to have semi-Poisson level spacings [3]. Critical statistics are predicted to be a generic feature [2] of these and other types of non-KAM systems. Multifractal behaviour has been demonstrated for Cantor spectra [6] where the level density itself is not smooth. However, until now, critical statistics have not been seen – and were not thought to be relevant to KAM systems.

These are systems ubiquitous in many areas of physics – where the transition to chaos, as a perturbing parameter is increased, is quite gradual.

Atoms in optical lattices subjected to pairs of pulses of finite duration were recently shown to provide a good experimental example of transport through a cantorus [7]; however, that system is integrable except around $p=0$. Further experiments using instead pairs of 'near-kicks', showed that the 2-kicked rotor (2-KR) has a more uniform classical phase space, with fully chaotic regions sandwiched between 'trapping regions', where the classical trajectories stick [8]; this more uniform phase-space permitted a generic, fully analytical treatment of the anomalous classical diffusion, without any detailed study of the classical phase-space.

We show here that the 2-KR enables us to finally isolate the signatures of fractal partial classical barriers in the eigenvalue statistics of a KAM system. We identify critical statistics at a localization-delocalization border, which can be compared with the MIT. This critical region has linear variances, with a slope related to the fractal scaling of the wavefunctions. Surprisingly, the level-spacings, $P(s)$, take an intermediate form, invariant over the critical regime, which is neither semi-Poissonian nor approaches the GOE form.

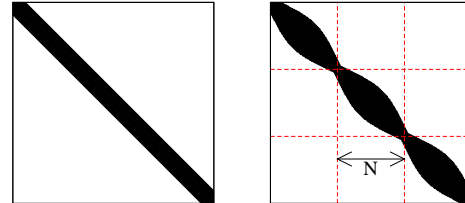


FIG. 1: Left (a): Structure of time-evolution matrix $U(T;0)$ for the Quantum Kicked Rotor (QKR), in a basis of momentum states, exemplifying the structure of a Band Random Matrix (BRM). Right (b): $U(T;0)$ for our system, the 2-KR, showing a characteristic 'pinching' of the band at the trapping momenta (dashed lines) which coincide with fractal classical phase-space barriers. Before delocalization, eigenstates are confined within a single momentum cell of dimension N .

Cantori are the fractal remnants of broken tori, which result at the end of a sequence of torus-breaking stipulated by the well-known KAM theorem [9]. The most robust cantori were found to result from the break-up of tori with winding numbers given by the golden ratio $R = (\sqrt{5} - 1)/2$. The corresponding classical and quantum transport has been extensively studied in the Quantum Kicked Rotor (QKR) and other standard KAM systems [10, 11, 12]. But these studies concern the properties of the phase-space local to the golden ratio cantorus. The cantori are embedded in a phase-space still substantially covered with stable islands. Hence signatures of the classical fractal structure in the spectral fluctuations are masked by localization of quantum states on different stable structures with different scaling characteristics. Below, we use the term critical statistics to make a clear distinction between the intermediate statistics analogous to those found in disordered and chaotic systems and the intermediate mixed-phase space statistics observed widely in systems for which a significant fraction of classical phase-space is covered by stable islands. The latter are also of much current interest eg [13]. However, in the 'critical' regime we study here, stable islands occupy 0.1% of total classical phase-space area so their influence is negligible.

The extensively studied Hamiltonian of the QKR, $H(x; p) = \frac{p^2}{2} + K \sin x_n (t - nT)$, involves a sequence of time-periodic 'kicks' (with period T) applied to a particle. The implementation using cold atoms in optical lattices [14] has provided a convincing demonstration of the quantum chaos phenomenon of Dynamical Localization see [15] and references therein. The 2-KR involves the modification of applying pairs of pulses. The modified kick potential is $V(x; t) = K \sin x_n (t - nT) + (t - nT + \dots)$; we have a short time interval between the kicks in each pair; we have a much longer time $T' = T$ between the pairs themselves. In experiments $0.01 < \sim < 1$ and $\sim' = 2$ in the usual re-scaled units [8]. The results are quite insensitive to \sim , but we take $T = 2$ so the average time per kick equals 1.

A study of the spectral fluctuations of a time-periodic system involves a study of the Floquet states and eigenphases, ie the eigenstates and eigenvalues of the one-period time-evolution operator $U(T; 0)$ [16]. For the QKR, the matrix representation, in a plane wave basis $|j\rangle$, has elements $U_{jm} = U_1^{\text{free}}: U_{jm}^{\text{kick}} = \exp i\frac{p^2}{2}T \sim = 2 : J_{1m}(\frac{K}{\sim})$. The 'kick' terms, $J_{1m}(\frac{K}{\sim})$ are ordinary integer Bessel functions and give the matrix the sharply banded form illustrated in Fig.1(a), since $J_b(\frac{K}{\sim}) \approx 0$ for $b > K \sim$. The 'free-evolution' term, approximately randomize the relative phases of the plane waves. Hence the resulting statistics correspond to those of Band Random Matrix Theory (BRMT) [16] rather than of RMT: ie if the dimensionality of the $U(T; 0)$ matrix we diagonalize is N_{tot} , the statistics are Poissonian for $N_{\text{tot}} > > b$; the eigenstates of the BRMT are exponentially localized in l , with a localization length in

momentum ($p = l\sim$) which equals $L_p \sim K^2 \sim$, so states separated in p by $> > L_p$ will be largely uncorrelated.

For the 2-KR, the corresponding matrix elements may be written as $U_{lm} = U_1^{\text{free}}: U_{lm}^{\text{2 kick}} = \exp i\frac{p^2}{2}T \sim = 2 : J_{1k}(\frac{K}{\sim}) J_{1m}(\frac{K}{\sim}) \exp i\frac{K^2}{2} \sim$. We have a free-evolution term corresponding to the evolution between kick pairs which, like the QKR, provides a near-random phase-shift between the plane waves. It is insensitive to the value \sim (excluding quantum-resonance regimes when \sim is a rational multiple of π). The term in the summation represents the total effect of the kick-pair and the small time interval \sim . As \sim is small, the k th waves can combine coherently. It is easy to see that $U_{lm}^{\text{2 kick}}$ is invariant if the products $K = K$ and $\sim = \sim$ are kept constant. Since $U(T; 0)$ is insensitive to \sim , we can mostly restrict ourselves to the two scaled parameters K and \sim , rather than to vary K and \sim independently.

The corresponding classical diffusion was studied in [8]: the consecutive kicks cancel form momentum $p' (2n+1) = \sim$ generating momentum-trapping regions permitted by broken phase-space barriers. The diffusion correlations which control transport through these regions, indeed depend only on K . Classical phase-space is periodic in p and partly partitioned into equal 'cells' of width $p = 2\pi/K$. The corresponding band-structure of U is illustrated in Fig.1(b): the band oscillates as shown, and U is approximately partitioned into sub-matrices of dimension $N = \frac{2\pi}{K}$ corresponding to the momentum cells. At the centre of the cells, classical diffusion rates are of the same order as the KR, so localization lengths $L_p \sim K^2 \sim$, for eigenstates well away from the trapping regions.

The key to our work is our ability to vary the coupling between the cells (eg by opening/closing the classical fractal 'gates' between them) separately from $b = N$, the degree of filling of each individual cell. We begin by defining a localized limit, where $b \ll N$ and $L_p \ll N \sim = \frac{2\pi}{K}$. It is clear that most states feel no constraint and this limit is Poissonian.

If we increase $K^2 \sim$ but have negligible coupling between cells, we approach the limit $b = N$! 1. Then for all eigenstates, $L_p \sim N \sim$ as the probability for all states gradually fills the cell uniformly. At the other extreme, if we allow strong coupling between cells, we move to yet another limit, as an increasing proportion of eigenstates become delocalized over several cells. The oscillatory structure of the band is lost and this limit regains the characteristics of the QKR. For $N_{\text{tot}} > > b = N$ this delocalized limit is also Poissonian [18].

We are interested in the transition regime between these localized and delocalized Poisson limits, as a function of the permeability of the fractal 'gates'. The regime of classical interest here is approximately $0.2 < K < 0.7$. Much below $K \sim 0.2$, the cantori close and classical phase-space becomes regular. Above $K \sim 0.7$, the cantori become too 'open' to provide effective barriers.

We investigated the corresponding quantum transport by evolving many wavepackets (initially centred on

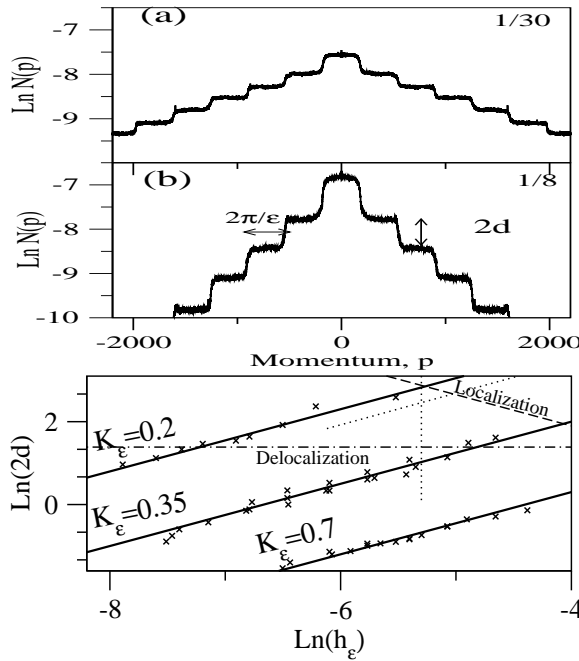


FIG. 2: Fig(a)–Final ($t = 1$) momentum distributions, $N(p)$, (slightly smoothed) for quantum wavepackets of the 2-QKR for $K = 20$, $\sim = 0.0175$ and $\sim = 1/8$ and $1/30$ respectively. $N(p)$ for both the eigenstates and wavepackets shows a long-range tail of ‘staircase’ form which on average follows the exponential $N(p) \propto \exp[-2(p - \bar{p})/L_p]$ where $L_p = N \sim = 2d$; since $N \sim = 2 = \sim$, the \sim -dependence of L_p is determined by the drop in probability, d , at each successive set of cantori. The first 3 steps of the staircase can be seen in experiments with optical lattices [7, 8]. Figure (b) shows that $\ln(2d)$ plotted against $\ln(\sim)$ lies on straight lines of invariant $K = K_\epsilon$, with constant slope 0.75. Hence $d/\sim^{0.75}$ and $L_p/\sim^{0.75}$ – in contrast to the well-known QKR result L_p/\sim^1 . The localization border ($K^2 = 2$) is shown by the dashed line. The delocalization border ($d' = 2$) is the dot-dash line. Critical statistics are found between these borders and are presented later in Fig 3 for points corresponding to the dotted lines.

$p = 0$) for a range of K and \sim , for long enough that the momentum spreading is arrested by dynamical localization. The resulting momentum probability distributions have a characteristic ‘staircase’ structure, shown in Fig 2(a). At each step, there is a steep drop in probability $N(p)_+ = e^{-2d}N(p)$ (where $N(p)$ represent probabilities before(–) and after(+) the step) concentrated over a narrow region ($1=6$ of a cell in every case) corresponding closely to the classical region permeated by cantori. The staircase tracks an exponential envelope $N(p) \propto \exp[-2(p - \bar{p})/L_p]$, where $L_p = \sim/d$. We average over several steps, to obtain d as a function of K and \sim . In Fig 2(b) we show that quite accurately, $d/\sim^{0.75} = f(K_\epsilon)$ where $f(K_\epsilon)$ is some function of the scaled kick-strength, K_ϵ . As an estimate, we obtain $d' = \sim^{0.75}/(3.5K_\epsilon^3)$ and use this to place the localization border. The inner steps of the staircase are seen in the momentum distributions of atoms in

optical lattices [7, 8]; so, though existing data is not in the critical regime, in principle the form of d is experimentally verifiable. A similar fractal dimension was obtained from the second moment of eigenstate wavefunctions, by a box counting procedure used in eg [5]. We find that the exponents for individual eigenstates fluctuate around $D_2' = 0.75$.

Note that the usual definition of the localization length of a wavepacket or eigenstate is given from the variance, $L_p = \langle p^2 \rangle - \langle p \rangle^2$. For the 2-QKR $L_p' = \sim$ if most of the probability lies a single cell uniformly. For the staircase exponential-localization of the 2-QKR, we found $L_p' = (d')^2 \sim = L_p$. Hence it may be useful to distinguish between the momentum variance L_p and the long-range localization length of the staircase, L_p . For the QKR, with a smooth exponential distribution, of course $L_p = L_p'$.

We have also obtained a large number of eigenstates and eigenvalues in the critical regime – the region in Fig 2(b) with $K_\epsilon > 0.2$, bounded by the localization border $K^2 = 2$ and the delocalization border $d' = 2$. Unitary ($T = 0$) was diagonalized in a symmetrized plane wave basis. Matrices with $N_{\text{tot}} = 10,000$ were diagonalized over different momentum ranges to obtain many cells in the range $1 = 0 \dots 100,000$. The individual eigenstates also all have a staircase structure at long-range, characterised by L_p . In the critical regime, typical eigenstates have a variance, $L_p = \sim = >> 1$ but there can be a very few eigenstates localised in the cantoral regions with $L_p = 1$. These disappear as the delocalization border $d' = 2$ is reached. We have verified that removing them has no appreciable effect on the statistics.

By taking $d' = 2$ as the onset of delocalization, we ensure almost all states in the critical regime had over 98% of their probability contained within a single cell. We then assigned the i th eigenstate to the n th cell if $(2n + 1) = \sim < p > (2n + 3) = \sim$. Once delocalization sets in, and states become spread over several cells, this procedure can fail to assign states meaningfully, but in this case the statistics revert back to the Poisson limit. The cells each contained (depending on \sim) 500–3000 eigenstates and corresponding eigenvalues. We averaged over 20–100 cells to obtain good statistics and used 12,000–70,000 eigenvalues for each spectrum.

In Fig 3(a), the $\chi^2(L)$ statistics are presented. These represent the variances in the spectral number density, $\chi^2(L) = \langle L^2 \rangle - \langle L \rangle^2$, where we consider a stretch of the spectrum with an average $\langle L \rangle$ levels. We found a linear form, $\chi^2(L) \propto L$, in the critical regime for $1 \ll L \ll L_{\text{cell}}$. The upper limit is needed since each cell contains nearly exactly $L_{\text{cell}} = \frac{2}{\sim}$ states. A straight line was fitted to the range $L = 5 \dots 40$ to obtain the slope – for all points except for the very largest values of $\sim = 1 \dots 4$, where a fit to the smaller range $L = 5 \dots \frac{2}{30 \sim}$ was used. The insets plot the values of calculated along the vertical dotted line of Fig 2(b) (left inset) and the diagonal line (right inset). They show a limiting slope ~ 0.125 , the closest to GOE the statis-

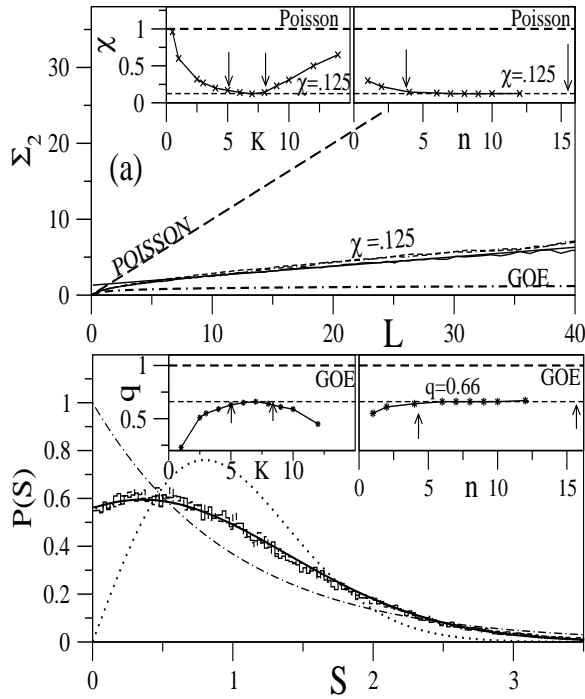


FIG. 3: Fig. (a) shows the variances $\Sigma^2(L)$ statistics and the form $\Sigma^2(L) = 0.125L$ in the critical regime, corresponding to a slope $\chi = 1=2(1 - D_2)$ where $D_2 = 0.75$ is the fractal dimension obtained from the wavefunctions. The insets plot along the dotted line cuts in Fig. 2. The arrows indicate the localization and delocalization borders respectively: critical statistics are seen in between. In the right insets, $n = \sim 1$. Fig. (b) shows the corresponding NNS distribution seen everywhere in the critical regime. Two histograms each using about 50,000 eigenvalues are plotted (with $K = 7$; $\sim 1=200$, 40 cells of about 1250 states and $K = 9$; $\sim 1=400$, 20 cells of 2500 states) showing that the results are insensitive to the cell size. The fit to a Berry-Robnik distribution is also shown, for $q = 0.66$. The insets show that a value of $q = 0.66$ is obtained between the localization and delocalization arrows.

tics get, is reached within the localization-delocalization

region. This value corresponds to the relation seen in the M II, $\chi = 1=2(1 - D_2)$ with $D_2 = 0.75$ and spatial dimension of one.

In Fig. 3 (b), corresponding nearest spacings distribution (NNS) are shown. Histograms obtained for two different cell sizes, are indistinguishable, indicating that the degree of 'binning' does not affect the results. They represent a distribution which, surprisingly, is clearly neither close to GOE nor semi-Poisson. A best fit to the well-known Berry-Robnik (BR) distribution [17] is also shown with a parameter $q = 0.66$. In a mixed phase-space system, in the semiclassical limit, q indicates the fraction of phase-space which is chaotic. Yet here 99.9% of the classical phase-space area is chaotic: the fractal trapping regions mimic the effects of stable islands covering 1=3rd of phase-space. While the BR distribution gives excellent results, the fit to a Brody distribution gives rather poor results, due to the absence of short-range repulsion. However, the $q = 0.66$ fit in a fully chaotic dynamical regime motivates further theoretical development.

In sum, in the critical regime, just before delocalization, classical trajectories are trapped within a momentum cell for extremely long times, but are all able to explore the fractal trapping regions which border the cell. The corresponding typical quantum eigenstates are also extended over—but essentially confined within—one cell. Without the tori/stable islands of a mixed phase-space system to exclude them from parts of phase space, they can sample the fractal regions (more or less) democratically. Hence the fractal ‘ngerprint’ becomes a global property of the full quantum spectrum, rather than of a local subset of states. This enables us to demonstrate, for the first time, that critical statistics—in particular the relation between fractal dimension D_2 and the level number ($\Sigma^2(L)$) statistics—can be a feature of a KAM system. A further insight is that this does not require cantori to be uniformly distributed over phase-space (as in pseudo-integrable billiards [3]): we conclude that it may suffice that typical trajectories all spend a long time trapped in the fractal regions.

This work was supported by the EP SRC.

[1] J.T. Chalker, I.V. Lerner, R.A. Smith, Phys. Rev. Lett. 77, 554 (1996); V.E. Kravtsov and K.A. Muttalib, Phys. Rev. Lett. 79, 1913 (1997).
[2] A.M. Garcia-Garcia and J.J.M. Verbaarschot, Phys. Rev. E 67, 046104 (2003).
[3] E.B. Bogomolny, U. Gerland and C. Schmit, Phys. Rev. E 59, R1315 (1999).
[4] D. Braun, G. Montambaux and M. Pascaud, Phys. Rev. Lett. 81, 1062 (1998).
[5] B. Huckestein and L. Schweitzer, Phys. Rev. Lett. 72, 713 (1994).
[6] T. Geisel, R. Ketzmerick, and G. Petschel, Phys. Rev. Lett. 69, 695 (1992).
[7] K. Vant, G. Ball, H. Ammann, N. Christensen, Physical Review E 59, 2846 (1999).
[8] P.H. Jones, M. Stocklin, G. Hur, T.S. Monteiro, Phys. Rev. Lett. 93, 223002 (2004).
[9] E. Ott, ‘Chaos in dynamical systems’, Cambridge University Press (1993).
[10] T. Geisel, G. Radons and J. Rubner, Phys. Rev. Lett. 57, 2883 (1986).
[11] S. Ishman, D.R. Gammel, R.E. Prince, Phys. Rev. A 36, 289 (1987).
[12] N.T.M.aitra and E.J. Heller, Phys. Rev. E 61, 3620 (2000).
[13] R. Ketzmerick, L. Hufnagel, F. Steinbach and M. Weiss, Phys. Rev. Lett. 85, 1214 (2000).

- [14] F.L. Moore, J.C. Robinson, C.F. Bharucha, B. Sundaram, M.G. Raizen, Phys. Rev. Lett. 75, 4598 (1995).
- [15] G. Casati, B.V. Chirikov, F.M. Izraelev, J. Ford, in "Lecture notes in Physics", Springer, Berlin, 93, 334 (1979); S. Fishman, D.R. Gremel, R.E. Prange, Phys. Rev. Lett. 49, 509 (1982).
- [16] F.M. Izraelev, Phys. Rep. 196, 299 (1990).
- [17] M.V. Berry and M. Robnik, J. Phys. A, 17, 669 (1986).
- [18] Note that these states are not fully delocalized in the sense of the Anderson transition: we still have a band Random Matrix, but with a wider band.